A Low Complexity Expectation Propagation Algorithm for Active User Detection for Massive Connectivity

Rui Ma, Yuanli Ma, Jikun Zhu, Zheng Wang
School of Information Science and Engineering
Southeast University, Nanjing, China
Email: ruima@seu.edu.cn, wznuaa@gmail.com

Yuekai Cai
Key Laboratory of Universal Wireless Communications
Beijing University of Posts and Telecommunications, Beijing, China
Email: echo-cai@bupt.edu.cn

***Abstract*—As the scale of Internet of Things (IoT) grows rapidly, accurate active user detection has emerged as an important problem in massive connectivity scenarios. This paper presents a novel low-complexity expectation propagation (LC-EP) algorithm for massive connectivity. Different from traditional methods that reduce the complexity of EP through channel hardening, LC-EP exploits a new statistical convergence property of the Gram matrix for the complexity reduction. Meanwhile, the decision method is modified from the original log-likelihood ratio (LLR)-based approach to an order-based method for the future performance gain. Simulation results demonstrate that the proposed LC-EP algorithm improves both detection accuracy and efficiency.**

***Index Terms*—Massive connectivity, active user detection, expectation propagation, low complexity.**

I. Introduction

In wireless communication networks, the multiple access technique is crucial for enabling IoT users to connect to the system simultaneously [1]. However, as the scale of connectivity is rapidly increasing, between 10^4 to 10^6 IoT devices need to be connected [2]. Nevertheless, in these scenarios, only a limited number of users are active during any given coherence interval [3]. Due to this irregular activation, it is essential for the base station (BS) to accurately identify the active users [4]. This challenge can be effectively addressed via a compressed sensing (CS) framework for sparse signal recovery, which has inspired the development of numerous CS-based algorithms for active user detection in such systems [5].

Among these, the EP algorithm in [6] achieves superior performance compared to other algorithms, such as approximate message passing (AMP) in [7], orthogonal matching pursuit (OMP) in [8] and group orthogonal matching pursuit (GOMP) algorithm in [9]. However, EP also suffers from the high complexity cost due to the matrix inversion required at each iteration. To mitigate this issue, traditional methods attempt to reduce complexity by eliminating the need for matrix inversion by leveraging channel hardening [10]. Unfortunately, such a manner is no longer applicable in massive connectivity scenarios, where the number of users significantly exceeds the pilot length, resulting in a lack of channel hardening property [11].

Corresponding author: Zheng Wang (email: wznuaa@gmail.com)

To overcome this limitation, in this work, we identify a novel statistical convergence property of the Gram matrix that facilitates complexity reduction. In addition, despite EP demonstrates excellent detection performance, the threshold derived from the traditional LLR test is not effective enough in accurately recovering the signal. Therefore, an order-based threshold is proposed to enhance decision performance of EP. Simulations show that LC-EP achieves competitive performance with lower complexity cost for massive connectivity.

II. EP algorithm for active user detection

We consider an uplink communication system in a single-cell massive connectivity scenario, where a BS with a single antenna serves N users, of which K are active [12]. The uplink channel coefficient from the n-th device to BS, denoted as h_n, follows independent Rayleigh fading: $h_n \sim \mathcal{CN}(0, \beta_n)$. The variance β_n represents the path-loss. Each active user transmits a pilot sequence of length L to BS. The received signal $\mathbf{y} \in \mathbb{C}^{L\times 1}$ at BS is then given by

$$\mathbf{y} = \sum_{n=1}^{N} \phi_n a_n h_n + \mathbf{w} = \mathbf{\Phi}\mathbf{x} + \mathbf{w}, \tag{1}$$

where $\phi_n \in \mathbb{C}^{L\times 1}$ is the pilot sequence of the n-th user. We adopt independent and identically distributed (i.i.d.) Gaussian pilot sequences and $\phi_{l,n} \sim \mathcal{CN}(0, \frac{1}{L})$. $\mathbf{\Phi} = [\phi_1, \ldots \phi_N] \in \mathbb{C}^{L\times N}$ is the pilot matrix. $a_n \in \{0, 1\}$ is the activity indicator of the n-th user, where $a_n = 1$ indicates that the user is active, and $a_n = 0$ indicates inactivity. $\mathbf{x}$ is the composite of activity vector a_n and channel vector h_n and $\mathbf{x} = \mathbf{a} \circ \mathbf{h} = [x_1, x_2, \ldots, x_N]^H$, where $x_n = a_n h_n$ and $\circ$ denotes the Hadamard product. $\mathbf{w} \in \mathbb{C}^{L\times 1} \sim \mathcal{CN}(\mathbf{0}, \sigma_w^2\mathbf{I})$ is additive white Gaussian noise (AWGN). The transmit power of all devices is ρ.

The goal of BS is to detect active users by recovering $\mathbf{x}$ from the noisy observation $\mathbf{y}$, for which the maximum a posteriori (MAP) probability estimator is commonly employed [13]. In particular, the output of the MAP estimator is given by

$$\hat{\mathbf{x}} = \arg\max_{\mathbf{x}\in\mathbb{C}^N} p(\mathbf{x}|\mathbf{y}) = \arg\max_{\mathbf{x}\in\mathbb{C}^N} p(\mathbf{y}|\mathbf{x})p(\mathbf{x}), \tag{2}$$

with

$$p(\mathbf{y}|\mathbf{x}) = \mathcal{CN}(\mathbf{y}|\mathbf{\Phi}\mathbf{x}, \sigma_w^2\mathbf{I}), \tag{3}$$

$$p(\mathbf{x}) = \prod_{n=1}^{N} \left[(1-\epsilon)\delta(x_n) + \epsilon \mathcal{CN}(x_n|0,\beta_n)\right]. \quad (4)$$

Here, $p(\mathbf{x})$ is the prior distribution and ϵ is the activity probability [14]. However, the optimization problem in (2) is computationally difficult due to the discrete nature of the activity vector $\mathbf{a}$. To address this, a proposal distribution $q(\mathbf{x})$ is given in [16] to approximate the target distribution $p(\mathbf{x}|\mathbf{y})$.

$$q(\mathbf{x}) = \mathcal{CN}(\mathbf{x}|\tilde{\mathbf{m}}, \tilde{\mathbf{V}}), \quad (5)$$

with

$$\tilde{\mathbf{V}} = \left(\sigma_w^{-2}\mathbf{\Phi}^H\mathbf{\Phi} + \tilde{\mathbf{V}}_1^{-1}\right)^{-1}, \quad (6)$$

$$\tilde{\mathbf{m}} = \tilde{\mathbf{V}}\left(\sigma_w^{-2}\mathbf{\Phi}^H\mathbf{y} + \tilde{\mathbf{V}}_1^{-1}\tilde{\mathbf{m}}_1\right), \quad (7)$$

where $\tilde{\mathbf{m}}_1$ and $\tilde{\mathbf{V}}_1$ belong to the approximated prior distribution $q_{\text{prior}}(\mathbf{x}) \triangleq \mathcal{CN}(\mathbf{x}|\tilde{\mathbf{m}}_1, \tilde{\mathbf{V}}_1)$. In this way, the mean vector of $q(\mathbf{x})$ accounts for the solution of problem in (2), i.e., $\hat{\mathbf{x}} = E_{q(\mathbf{x})}[\mathbf{x}] = \tilde{\mathbf{m}}$. To obtain the solution $\tilde{\mathbf{m}}$, EP has been introduced to update the pairs $(\tilde{\mathbf{m}}_1^i, \tilde{\mathbf{v}}_1^i)$ in each i-th iteration using the following steps [15].

First, compute the cavity marginal distribution $q^i_{\backslash \text{prior},n}(x_n)$.

$$q^i_{\backslash \text{prior},n}(x_n) = \frac{q_n^i(x_n)}{q^i_{\text{prior},n}(x_n)} = \mathcal{CN}(x_n|\tilde{m}^i_{\backslash 1,n}, \tilde{v}^i_{\backslash 1,n}), \quad (8)$$

where

$$\tilde{v}^i_{\backslash 1,n} = \left[\left(\tilde{V}^i_{nn}\right)^{-1} - \left(\tilde{v}^i_{1,n}\right)^{-1}\right]^{-1}, \quad (9)$$

$$\tilde{m}^i_{\backslash 1,n} = \tilde{v}^i_{\backslash 1,n}\left[\left(\tilde{V}^i_{nn}\right)^{-1}\tilde{m}^i_n - \left(\tilde{v}^i_{1,n}\right)^{-1}\tilde{m}^i_{1,n}\right]. \quad (10)$$

Next, compute the mean $E_q^i[x_n]$ and variance $V_q^i[x_n]$ of $\hat{q}_n^i(x_n)$, where $\hat{q}_n^i(x_n) = p(x_n)q^i_{\backslash \text{prior},n}(x_n)$.

$$E_q^i[x_n] = \frac{X^i_{1,n}}{X^i_{0,n}}, \quad (11)$$

$$V_q^i[x_n] = \frac{X^i_{2,n}}{X^i_{0,n}} - \left|E_q^i[x_n]\right|^2, \quad (12)$$

where $X^i_{m,n}$ (with $m = 0,1,2$) represents the moments of $\hat{q}_n^i(x_n)$, which can be computed as follows [17].

$$X^i_{0,n} = (1-\epsilon)\mathcal{CN}\left(0|\tilde{m}^i_{\backslash 1,n}, \tilde{v}^i_{\backslash 1,n}\right) + \epsilon\mathcal{CN}\left(0|\tilde{m}^i_{1,n}, \beta_n + \tilde{v}^i_{\backslash 1,n}\right), \quad (13)$$

$$X^i_{1,n} = \epsilon\mathcal{CN}\left(0 \mid \tilde{m}^i_{\backslash 1,n}, \beta_n + \tilde{v}^i_{\backslash 1,n}\right)\frac{\tilde{m}^i_{\backslash 1,n}\beta_n}{\beta_n + \tilde{v}^i_{\backslash 1,n}}, \quad (14)$$

$$X^i_{2,n} = \epsilon\mathcal{CN}\left(0|\tilde{m}^i_{\backslash 1,n}, \beta_n + \tilde{v}^i_{\backslash 1,n}\right)\left(\left|\frac{\tilde{m}^i_{\backslash 1,n}\beta_n}{\beta_n + \tilde{v}^i_{\backslash 1,n}}\right|^2 + \frac{\beta_n\tilde{v}^i_{\backslash 1,n}}{\beta_n + \tilde{v}^i_{\backslash 1,n}}\right). \quad (15)$$

Finally, update the pairs $(\tilde{\mathbf{m}}_1^i, \tilde{\mathbf{v}}_1^i)$ such that $\hat{q}_n^{i+1}(x_n)$ has the same mean and variance with $q_n^{i+1}(x_n)$

$$\tilde{v}^{i+1}_{1,n} = \left[V_q^i[x_n]^{-1} - \left(\tilde{v}^i_{\backslash 1,n}\right)^{-1}\right]^{-1}, \quad (16)$$

$$\tilde{m}^{i+1}_{1,n} = \tilde{v}^{i+1}_{1,n}\left[V_q^i[x_n]^{-1}E_q^i[x_n] - \left(\tilde{v}^i_{\backslash 1,n}\right)^{-1}\tilde{m}^i_{\backslash 1,n}\right]. \quad (17)$$

Once the EP algorithm converges, the LLR test is used to identify the active device. For hypothesis testing, where H_0 represents an inactive user and H_1 denotes an active user, the LLR-based detector is given by

$$\text{LLR}(\hat{x}_n) = \log\left(\frac{p_{\hat{x}_n|a_n}(\hat{x}_n \mid a_n \neq 0)}{p_{\hat{x}_n|a_n}(\hat{x}_n \mid a_n = 0)}\right) \underset{H_0}{\overset{H_1}{\gtrless}} 0, \quad (18)$$

which is further simplified based on the threshold θ_n as given by [6]

$$|\hat{x}_n|^2 \underset{H_0}{\overset{H_1}{\gtrless}} \theta_n = \log\left(1 + \frac{\beta_n}{\tilde{V}_{nn}}\right) \Big/ \left(\frac{1}{\tilde{V}_{nn}} - \frac{1}{\beta_n + \tilde{V}_{nn}}\right). \quad (19)$$

III. Complexity reduction

The matrix $\mathbf{\Phi}$ in massive connectivity scenario has a dimension of $L \times N$, $N > L$, where both N and L approach infinity. As a result, $\mathbf{\Phi}$ is a wide matrix, in contrast to the tall matrix typically encountered in conventional massive MIMO systems. In this case, an important statistical convergence property of the Gram matrix is leveraged to facilitate complexity reduction, as elaborated in the following discussion.

Theorem 1. *Let $\mathbf{\Phi} \in \mathbb{C}^{L\times N}$ be a matrix whose entries satisfy $\phi_{l,n} \sim \mathcal{CN}\left(0, \frac{1}{L}\right)$. Define $\mathbf{G} = \mathbf{\Phi}^H\mathbf{\Phi}$ as the corresponding $N \times N$ Gram matrix. As the number of rows L tends to infinity, $\mathbf{G}$ converges numerically to the identity matrix. Specifically, we have*

$$\begin{aligned} &\text{E}(\mathbf{G}_{kk}) = 1 \quad \textit{and} \quad \lim_{L\to\infty}\text{Var}(\mathbf{G}_{kk}) = 0, \\ &\lim_{L\to\infty}\text{E}(\mathbf{G}_{kj}) = 0 \quad \textit{and} \quad \lim_{L\to\infty}\text{Var}(\mathbf{G}_{kj}) = \frac{1}{2} \quad (k \neq j). \end{aligned} \quad (20)$$

Proof: For a better understanding, the matrix $\mathbf{\Phi}$ and its Hermitian transpose $\mathbf{\Phi}^H$ are represented as follows

$$\mathbf{\Phi} = \begin{pmatrix} \phi_{11} & \cdots & \phi_{1N} \\ \vdots & \ddots & \vdots \\ \phi_{L1} & \cdots & \phi_{LN} \end{pmatrix}, \quad \mathbf{\Phi}^H = \begin{pmatrix} \phi_{11}^* & \cdots & \phi_{L1}^* \\ \vdots & \ddots & \vdots \\ \phi_{1N}^* & \cdots & \phi_{LN}^* \end{pmatrix}$$

The k-th diagonal element of $\mathbf{G}$ is computed as the sum of L terms, which can be expressed as

$$\mathbf{G}_{kk} = \sum_{l=1}^{L}|\phi_{lk}|^2 = \phi_{1k}^*\phi_{1k} + \phi_{2k}^*\phi_{2k} + \cdots + \phi_{Lk}^*\phi_{Lk}. \quad (21)$$

Given that each element ϕ_{lk} follows a normalized complex Gaussian distribution, i.e., $\phi_{lk} = a_{lk} + jb_{lk} \sim \mathcal{CN}(0, \frac{1}{L})$, the summation in (21) can be rewritten as the sum of $2L$ terms

$$\mathbf{G}_{kk} = \sum_{l=1}^{L} a_{lk}^2 + b_{lk}^2, \quad (22)$$

where $a_{lk}, b_{lk} \sim \mathcal{N}(0, \frac{1}{2L})$. By normalizing a_{lk} and b_{lk} to ${a_{lk}}'$ and ${b_{lk}}'$, where ${a_{lk}}', {b_{lk}}' \sim \mathcal{N}(0,1)$, we establish the relationships $a_{lk} = \frac{1}{\sqrt{2L}} \cdot {a_{lk}}'$ and $b_{lk} = \frac{1}{\sqrt{2L}} \cdot {b_{lk}}'$. Consequently, (22) becomes

$$\mathbf{G}_{kk} = \frac{1}{2L}\sum_{l=1}^{L} {a_{lk}}'^2 + {b_{lk}}'^2. \quad (23)$$

TABLE I
SUMMARY OF DIFFERENT PROPERTIES OF GRAM MATRIX

Dimension	Statistical Convergence Property	Asymptotic Orthogonality	Asymptotic Diagonal Dominance
N is fixed, $L \to \infty$ $(L \gg N)$	✓	✓	✓
L is fixed, $N \to \infty$ $(N \gg L)$	×	×	×
$N, L \to \infty$, $\frac{N}{L} = \beta \leq 1$	✓	×	×
$N, L \to \infty$, $\frac{N}{L} = \beta > 1$	✓	×	×

Since these terms are normalized and independent, $\mathbf{G}_{kk}$ follows a chi-squared distribution, i.e, $\mathbf{G}_{kk} \sim \frac{1}{2L}\chi^2(2L)$. Therefore, the expected value of the diagonal elements is 1, and the variance of $\mathbf{G}_{kk}$ is given by

$$\mathrm{Var}\left(\mathbf{G}_{kk}\right) = \left(\frac{1}{2L}\right)^2 \cdot 4L = \frac{1}{L}. \tag{24}$$

As L approaches infinity, the variance of $\mathbf{G}_{kk}$ asymptotically converges to 0.

On the other hand, the kj-th off-diagonal element, where $k \neq j$, is the sum of L independent terms

$$\mathbf{G}_{kj} = \sum_{l=1}^{L} \phi_{lk}\phi_{lj}^* = \phi_{1k}\phi_{1j}^* + \phi_{2k}\phi_{2j}^* + \cdots + \phi_{Lk}\phi_{Lj}^*. \tag{25}$$

Since ϕ_{lk} is independent of ϕ_{lj}^*, it follows that $\phi_{lk}\phi_{lj}^* \sim \mathcal{CN}(0, \frac{1}{2L})$. According to the central limit theorem, as L tends to infinity, the distribution of the normalized sample mean converges to a standard normal distribution, i.e.,

$$\frac{\mathbf{G}_{kj} - L\mu}{\sqrt{L}\sigma} \sim \mathcal{N}(0,1), \tag{26}$$

where μ is the mean of $\phi_{lk}\phi_{lj}^*$, which is 0, and σ is the standard deviation of $\phi_{lk}\phi_{lj}^*$, which is $\frac{1}{\sqrt{2L}}$. Therefore, the expected value of these off-diagonal terms approaches zero, and the variance of $\mathbf{G}_{kj}$ is $(\sqrt{L}\sigma)^2 = \frac{1}{2}$, thus completing the proof. ■

Note that this statistical convergence property is not equivalent to channel hardening, while channel hardening is actually a more strict property. A summary of different properties of Gram matrix is provided in *Table 1*. From *Table 1*, it can be concluded that statistical convergence holds as long as L tends to infinity, which confirms Theorem 1.

Benefiting from this, we can replace the Gram matrix $\mathbf{\Phi}^H\mathbf{\Phi}$ in (6) with its corresponding diagonal matrix $\mathbf{D}$, based on experimental results showing that the off-diagonal elements of $\mathbf{\Phi}^H\mathbf{\Phi}$ are nearly zero, making the impact on matrix processing negligible. Since the diagonal elements of $\mathbf{\Phi}^H\mathbf{\Phi}$ tend to 1, the k-th diagonal term of $\tilde{\mathbf{V}}$ can be simplified as

$$\tilde{V}_{kk} \approx \frac{1}{\sigma_w^{-2}\mathbf{I}_{kk} + \frac{1}{\tilde{\mathbf{V}}_{1,kk}}}, \tag{27}$$

where $\tilde{\mathbf{V}}_{1,kk}$ denotes the k th diagonal term of $\tilde{\mathbf{V}}_1$. By doing this, the complexity of updating $\tilde{\mathbf{V}}$ in (6) can be reduced from $\mathcal{O}(N^3)$ to $\mathcal{O}(N)$. The update of $\tilde{\mathbf{m}}$ in (7) has a complexity of $\mathcal{O}(N^2)$. Once the EP marginals $q_{\text{prior},n}^i(x_n)$ have been computed, the parallel update of pairs $(\tilde{\mathbf{m}}_1^i, \tilde{\mathbf{v}}_1^i)$ has a small computational complexity $\mathcal{O}(N)$.

The overall complexity of EP becomes $\mathcal{O}(IN^2)$, which is greatly smaller than $\mathcal{O}\left(ILN^2\right)$ in [6] if EP runs I iterations. The complexity comparisons among different algorithms is shown in *Table 2*.

IV. ORDER-BASED THRESHOLD ACTIVITY DETECTOR

In this section, an order-based threshold is introduced as a replacement for the original LLR threshold in order to further enhance performance. One of the key observations why EP outperforms other algorithms is EP's ability to create a clear distinction between active and inactive users. By recovering inactive user closer to zero, EP makes it easier to classify them accurately. However, the threshold used to determine user activity derived from the LLR test does not fully leverage this advantage in signal recovery.

Specifically, as can be seen in (19), the threshold θ_n is determined by two factors including the path loss of user n, β_n, and the variance of the output corresponding to each user, $\tilde{V}_{nn}$. A key observation is that θ_n exhibits a positive correlation with $\tilde{V}_{nn}$, i.e.,

$$\theta_n \propto \tilde{V}_{nn}. \tag{28}$$

To illustrate this relationship, we present a numerical example that shows how θ_n varies with $\tilde{V}_{nn}$ under different path loss values, β_n. In this example, we set β_n to values of 1×10^{-9}, 1×10^{-10}, and 1×10^{-11}, while $\tilde{V}_{nn}$ ranges from 1×10^{-15} to 1×10^{-13}. The corresponding variation in θ_n is shown in Fig. 1.

It has been observed that when $\tilde{V}_{nn}$ is smaller, θ_n also becomes smaller. This correlation introduces a challenge: Although EP yields smaller values $\tilde{m}_n$ in the case of inactive users, the corresponding values of $\tilde{V}_{nn}$ are also smaller according to (7), resulting in even smaller θ_n as illustrated in Fig. 2. From Fig. 2, the decision process becomes more difficult because of the relationship between $\tilde{m}_n$ and θ_n. Consequently, the LLR-based threshold in EP fails to well suit in signal recovery.

To address this issue, an ordered-based threshold method is proposed. Given the clear distinction in recovery values between active and inactive users, the K-th largest active signal can be directly used as a threshold. This approach enables precise classification of active and inactive users. To be more specific, this method involves first calculating the absolute estimated values $|\hat{x}_n|$ for all users and sorting them in descending order as follows

$$|\hat{x}_1| \geq |\hat{x}_2| \geq \cdots \geq |\hat{x}_N|. \tag{29}$$

TABLE II
COMPLEXITY COMPARISONS IN $L \times N$ MASSIVE CONNECTIVITY SCENARIOS OVER I ITERATIONS

	complexity order	32×128 massive connectivity	64×256 massive connectivity
OMP [8]	$\mathcal{O}(KLN)$	53248	425984
AMP-soft threshold [7]	$\mathcal{O}(ILN)$	16384	65536
EP [6]	$\mathcal{O}\left(ILN^2\right)$	2097152	16777216
LC-EP	$\mathcal{O}(IN^2)$	65536	262144

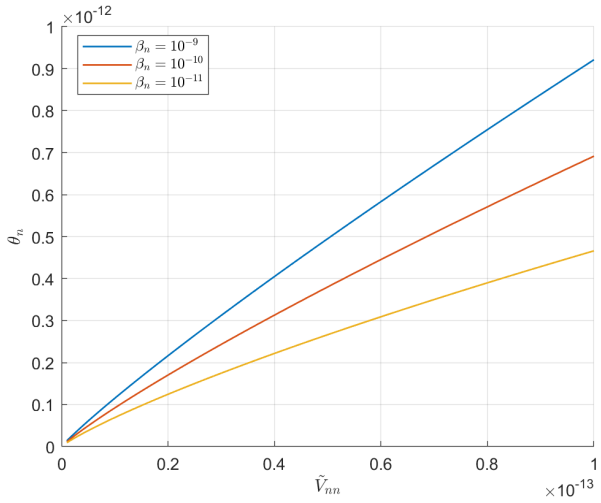

Fig. 1. Threshold θ_n versus $\tilde{V}_{nn}$ for different pathloss β_n.

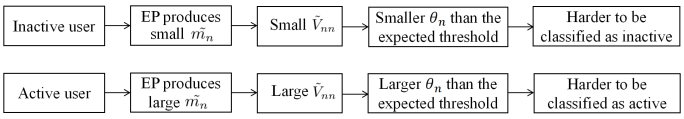

Fig. 2. The impact of θ_n on user activity classification.

Next, the K-th largest value, $|\hat{x}_K|$, is selected as the threshold, where K is the number of active users. As a result, the threshold is defined as $\theta = |\hat{x}_K|$. Users with estimated values smaller than this threshold are classified as inactive, while those with larger values are considered active. This classification is formalized as follows

$$\hat{a}_n = \begin{cases} 1 & \text{if } |\hat{x}_n| \geq \theta \\ 0 & \text{if } |\hat{x}_n| < \theta \end{cases}. \tag{30}$$

In summary, the proposed LC-EP algorithm is presented in Algorithm 1.

Algorithm 1 Low Complexity Expectation Propagation (LC-EP) Algorithm

Input: $\mathbf{y}$, $\mathbf{\Phi}$, β_n, σ_w^2, ϵ, $\tilde{\mathbf{m}}_1^0$, $\tilde{\mathbf{V}}_1^0$
Output: $\tilde{\mathbf{V}}$, $\tilde{\mathbf{m}}$, $\hat{a}_n$, $\forall n \in \{1, 2, \ldots, N\}$
for $i = 0, 1, 2, \ldots, I$ **do**
  compute $\tilde{\mathbf{V}}^{i+1}$, $\tilde{\mathbf{m}}^{i+1}$ by (27) (7)
  for $n = 1, 2, \ldots, N$ **do**
    compute $\tilde{v}_{\backslash 1,n}^{i+1}$, $\tilde{m}_{\backslash 1,n}^{i+1}$ by (9) (10)
    compute $X_{0,n}^{i+1}$, $X_{1,n}^{i+1}$, $X_{2,n}^{i+1}$ by (13), (14), (15)
    compute $E_q^{i+1}[x_n]$, $V_q^{i+1}[x_n]$ by (11) (12)
    compute $\tilde{v}_{1,n}^{i+1}$, $\tilde{m}_{1,n}^{i+1}$ by (16) (17)
  end for
end for
Threshold $\hat{\mathbf{x}}$ using the threshold θ in (30)

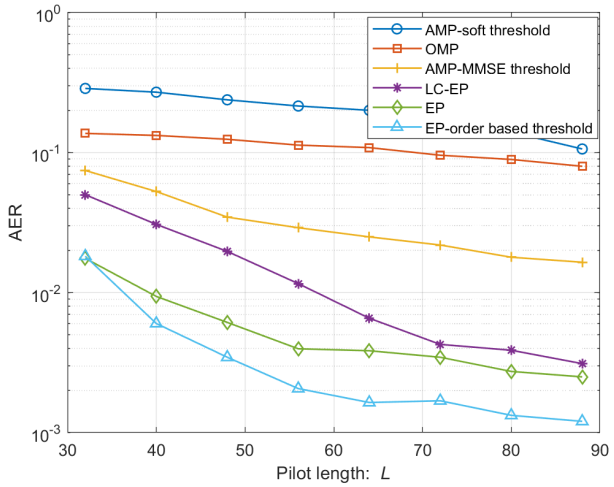

Fig. 3. Performance comparison of different methods based on AER versus increasing pilot length

V. NUMERICAL RESULTS

In our simulations, we consider a wireless communication system with $N = 128$ users, each utilizing an L-dimensional pilot sequence, where L is less than N. The pathloss of the wireless channel for the n-th user is modeled as $\beta_n = -128.1 - 36.7 \log_{10}(d_n)$ dB, where d_n represents the distance between the n-th user device and BS. The distance d_n is assumed to be randomly distributed within the range of 300 meters to 500 meters, capturing the variability in user locations in a typical wireless communication environment. The noise spectral density is set to -169 dBm/Hz, and the system operates with a transmission bandwidth of 1 MHz. The activity probability ϵ is set to 0.1, indicating that only 10% of users are active at any given time. The activity error rate (AER) is defined as the percentage of errors, which includes both missed detection and false alarms. To evaluate the performance of the proposed LC-EP detector, we compare its AER with several existing methods, including AMP with a soft-threshold denoiser [7], MMSE denoiser-based AMP [12], EP [6], and OMP [8].

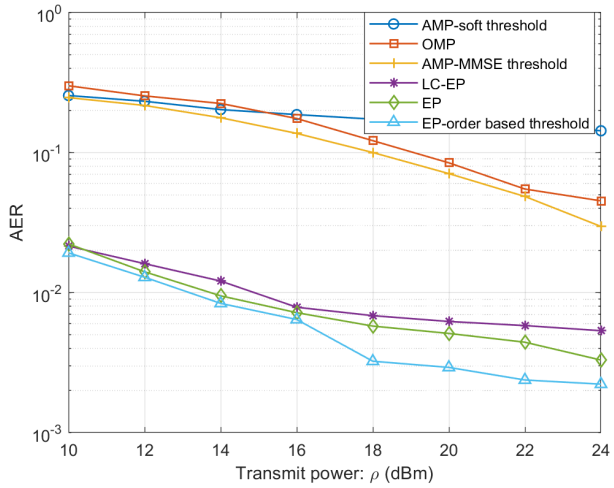

Fig. 4. Performance comparison of different methods based on AER versus increasing transmit power.

Fig. 3 illustrates the AER performance as the length of the pilot sequences L varies from 32 to 88. In this simulation, the transmit power is set to $\rho = 13\,\text{dBm}$. It can be observed that our proposed order-based threshold EP algorithm significantly outperforms the EP algorithm using LLR decision, demonstrating the advantages of order-based threshold EP in signal recovery. On the other hand, the proposed LC-EP algorithm, which is designed to reduce computational complexity, shows some degradation in performance compared to the EP algorithm [6]. However, as the pilot length L increases, the performance of LC-EP approaches that of EP. This is because, in this case, the Gram matrix becomes numerically closer to the identity matrix, which is consistent with the theoretical results outlined in Theorem 1.

Fig. 4 shows the AER performance of different algorithms when the transmit power ρ ranges from 10 to 24 dBm. The AER decreases with increasing transmit power for all methods. Among them, the EP-order based threshold algorithm exhibits the best performance. The LC-EP algorithm performs better than the others except for EP-order based threshold, though it shows slightly higher AER compared to the traditional EP method. The simulation results demonstrate that LC-EP achieves complexity reduction while maintaining a relatively small performance loss.

VI. Conclusion

This paper presents a novel LC-EP algorithm for active user detection in massive connectivity scenarios. By exploiting a unique statistical convergence property of the Gram matrix, the LC-EP algorithm successfully reduces computational complexity while maintaining detection performance. Additionally, an ordered-based threshold method is introduced to enhance the performance of the decision-making process compared to traditional LLR method. Simulation results confirm that the proposed LC-EP algorithm achieves a better trade-off between complexity and performance, especially as the pilot length increases. These results demonstrate the potential of the LC-EP algorithm in efficiently identifying active users for massive connectivity scenarios.

Acknowledgment

This work was supported in part by the National Key R&D Program of China under Grants No.2023YFC2205501, and in part by National Natural Science Foundation of China under Grants No.62371124.

References

[1] C. Bockelmann *et al.*, "Massive machine-type communications in 5G: Physical and mac-layer solutions," *IEEE Commun. Mag.*, vol. 54, no. 9, pp. 59-65, Sep. 2016.

[2] L. Liu, E. G. Larsson, W. Yu, P. Popovski, C. Stefanovic, and E. De Carvalho, "Sparse signal processing for grant-free massive connectivity: A future paradigm for random access protocols in the Internet of Things," *IEEE Signal Processing Mag.*, vol. 35, no. 5, pp. 88-99, 2018.

[3] X. LI, X. Gao, Y. Liu, G. Huang, M. Zeng, and D. Qiao, "Overlay CR-NOMA assisted intelligent transportation system networks with imperfect SIC and CEEs," *Chinese Journal of Electronics*, vol. 32, no. 6, pp. 1258–1270, 2023.

[4] K. Guo, R. Liu, C. Dong, K. An, Y. Huang, and S. Zhu, "Ergodic capacity of NOMA-based overlay cognitive integrated satellite-UAV-terrestrial networks," *Chinese Journal of Electronics*, vol. 32, no. 2, pp. 273–282, 2023.

[5] X. Chen, D. W. K. Ng, W. Yu, E. G. Larsson, N. Al-Dhahir, and R. Schober, "Massive access for 5G and beyond," *IEEE J. Select. Areas Commun.*, vol. 39, no. 3, pp. 615-637, 2020.

[6] J. Ahn, B. Shim, and K. B. Lee, "EP-based joint active user detection and channel estimation for massive machine-type communications," *IEEE Trans. Commun.*, vol. 67, no. 7, pp. 5178-5189, 2019.

[7] G. Hannak, M. Mayer, A. Jung, G. Matz, and N. Goertz, "Joint channel estimation and activity detection for multiuser communication systems," in *Proc. IEEE Int. Conf. Commun. Workshops*, Jun. 2015, pp. 2086-2091.

[8] J. A. Tropp and A. C. Gilbert, "Signal recovery from random measurements via orthogonal matching pursuit," *IEEE Trans. Inf. Theory*, vol. 53, no. 12, pp. 4655-4666, Dec. 2007.

[9] C. Bockelmann, H. F. Schepker, and A. Dekorsy, "Compressive sensing based multi-user detection for machine-to-machine communication," *IEEE Trans. Emerg. Telecommun. Technol.*, vol. 24, no. 4, pp. 389-400, 2013.

[10] X. Tan, Y.-L. Ueng, Z. Zhang, X. You, and C. Zhang, "A low-complexity massive MIMO detection based on approximate expectation propagation," *IEEE Trans. Veh. Technol.*, vol. 68, no. 8, pp. 7260-7272, 2019.

[11] L. Liu and W. Yu, "Massive connectivity with massive MIMO?Part II: Achievable rate characterization," *IEEE Trans. Signal Process.*, vol. 66, no. 11, pp. 2947-2959, 2018.

[12] L. Liu and W. Yu, "Massive connectivity with massive MIMO?Part I: Device activity detection and channel estimation," *IEEE Trans. Signal Process.*, vol. 66, no. 11, pp. 2933-2946, 2018.

[13] H. Zhu and G. B. Giannakis, "Exploiting sparse user activity in multiuser detection," *IEEE Trans. Commun.*, vol. 59, no. 2, pp. 454-465, Feb. 2011.

[14] J. M. Hernández-Lobato, D. Hernández-Lobato, and A. Suárez, "Expectation propagation in linear regression models with spike-and-slab priors," *Mach. Learn.*, vol. 99, no. 3, pp. 437-487, Jun. 2015.

[15] M. Opper and O. Winther, "Gaussian processes for classification: Mean-field algorithms," *Neural Comput.*, vol. 12, no. 11, pp. 2655-2684, Nov. 2000.

[16] T. P. Minka, "Expectation propagation for approximate Bayesian inference," in *Proc. 7th Conf. Uncertainty Artif. Intell.*, 2001, pp. 362-369, Seattle, WA, USA.

[17] J. Ahn, B. Shim, and K. B. Lee, "Expectation propagation-based active user detection and channel estimation for massive machine-type communications," in *Proc. IEEE Int. Conf. Commun. Workshops*, 2018, pp. 1-6, Kansas City, MO, USA.